

## Cone phase and magnetization fluctuations in Au/Co/Au thin films near the spin-reorientation transition

K. A. Seu,<sup>1,2</sup> S. Roy,<sup>2,\*</sup> J. J. Turner,<sup>3</sup> S. Park,<sup>4</sup> C. M. Falco,<sup>5</sup> and S. D. Kevan<sup>1</sup>

<sup>1</sup>*Department of Physics, University of Oregon, Eugene, Oregon 97403, USA*

<sup>2</sup>*Advanced Light Source, Lawrence Berkeley National Laboratory, Berkeley, California 94720, USA*

<sup>3</sup>*Department of Physics & Astronomy, Stony Brook University, Stony Brook, New York 11794, USA*

<sup>4</sup>*Department of Physics, Pusan National University, Busan 609735, Korea*

<sup>5</sup>*Optical Sciences Center, University of Arizona, Tucson, Arizona 85721, USA*

(Received 18 February 2010; revised manuscript received 25 June 2010; published 14 July 2010)

Using coherent soft x-ray scattering we have measured slow magnetization fluctuations in an Au/Co/Au heterostructure near a thermally driven spin-reorientation phase transition. The intermediate scattering function is well described by a stretched exponential, suggesting cooperative motion through the transition. The decay times were found to exhibit a pronounced maximum as a function of temperature. We argue that the transition proceeds through a cone phase in which the local magnetization evolves continuously from a perpendicular to longitudinal orientation. Our results demonstrate a different and fruitful way to probe the complex spatiotemporal dynamics that arise in unusual magnetic phases with competing anisotropies.

DOI: 10.1103/PhysRevB.82.012404

PACS number(s): 75.70.Kw, 75.30.Gw, 75.40.Gb

Competition between phases with similar free energy can lead to diverse nanoscale electronic and magnetic textures that dramatically impact material properties. For example, precise control of ferromagnetic thin film structure allows one to fine tune the magnetic anisotropies<sup>1–7</sup> to induce a thickness-driven or thermally driven spin-reorientation transition (SRT), wherein the lowest order anisotropy vanishes and the equilibrium magnetization direction changes from in-plane to out-of-plane.<sup>8</sup> The resulting dominance of higher order anisotropies near an SRT stabilizes a number of non-trivial domain states.<sup>1,9–11</sup> Recently, for example, a static “cone domain state” with locally canted spins was imaged in low anisotropy Co:Pt multilayers.<sup>12,13</sup> The cone state is predicted to play a key role in continuous, thermally driven SRTs and supports a class of fluctuating, nanoscale domain patterns.

Through combined application of resonant soft x-ray magnetic scattering and photon correlation spectroscopy to an epitaxial Au/Co/Au thin film heterostructure, we have accomplished the first x-ray measurements of magnetization fluctuations near a thermally driven SRT. At all temperatures and scattering wave vectors, we observe an intermediate scattering function that is well described by a stretched exponential functional form, indicative of collective motion. The decay time near the transition was found to be two to three times longer than that measured near the extrema of our temperature range. Previous measurements of the low-order anisotropy constants suggest that the transition is continuous and proceeds through a cone state in which the local magnetization evolves continuously from a perpendicular to a longitudinal orientation with increasing temperature. We ascribe the observed slowing to a flat free energy landscape of the cone phase and possibly to the formation of very small, fluctuating cone phase domains.

The sample used in the experiment was epitaxial Co whose structure is Si(111)/Cu 4 nm/Au 2 monolayer/Co 8 monolayer/Au 3.5 nm, grown via molecular beam epitaxy.<sup>7</sup> The magnetometry was performed by a superconducting

quantum interference device magnetometer. Figure 1(d) shows the magnetization as a function of temperature at an applied field of 10 Oe. The preferred magnetization direction lies in the plane of the film at  $T=300$  K and rotates out-of-plane as the temperature decreases to 150 K.

Coherent x-rays have been widely used to study the local in-plane configuration and dynamical behavior of a variety of systems ranging from polymers to magnetic materials.<sup>14–19</sup> Diffuse scattering of coherent x-rays give rise to speckle due to the interference of scattered wave fronts that are randomly phase shifted by the morphology of the

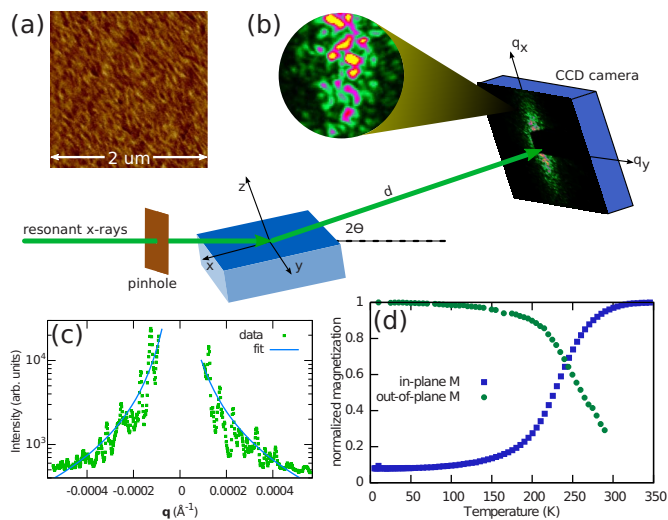


FIG. 1. (Color online) (a) MFM image of the sample at 300 K. The geometry for the resonant x-ray scattering experiment is shown in (b). Incident x-rays are filtered with a  $\sim 10$   $\mu\text{m}$  pinhole, creating a spatially coherent light source. The scattering pattern is collected with a CCD camera at an angle of  $2\theta=18^\circ$ . Detail of the speckle pattern is shown in the inset. Line cut of the data is shown in (c). The spin reorientation of the sample is illustrated by the SQUID curves in (d), where the magnetization changes from out-of-plane to in-plane as the temperature is increased.

sample, such as surface roughness. For magnetic systems probed with photons at an energy near an absorption edge, the speckle pattern will have an additional contribution from magnetic heterogeneity.<sup>16,17,19,20</sup> In the present case, any evolution in the magnetic morphology associated with the thermally driven SRT results in a change in the speckle pattern. The principle of x-ray photon correlation spectroscopy (XPCS) is to autocorrelate the intensity scattered into a single speckle as a function of time to probe the spatiotemporal character of the underlying material fluctuations.<sup>21</sup>

XPCS measurements were carried out at beamline 12.0.2.2 of the Advanced Light Source at Lawrence Berkeley National Laboratory.<sup>22</sup> The experiment was conducted in a small angle diffuse reflection geometry at a grazing incidence angle of  $9^\circ$  [Fig. 1(b)]. A coherent x-ray beam was obtained by placing a  $\sim 10 \mu\text{m}$  pinhole approximately 6 mm in front of the sample. A charge coupled device (CCD) placed 0.45 m downstream was used to record entire speckle patterns as a function of time. Magnetic contrast is provided by tuning the energy of the incoming linear  $\sigma$ -polarized x-rays to the  $L_3$  edge of Co (778 eV).<sup>23</sup> At resonance and in the dipole approximation, to leading order the signal is sensitive to magnetic moments which are orthogonal to the polarization. The net scattered intensity can then be written as  $I \propto |f_c|^2 + |f_m|^2$ , where  $f_c$  and  $f_m$  are the charge and magnetic scattering factors. Although the signal is a combination of charge and relatively weaker magnetic scattering, we assume that the charge scattering remains static in time, and any time variations were related to the dynamic feature of the magnetic structure. Indeed, time average of the data was found to retain speckle features arising due to constant charge background. The experiment was conducted by taking a long series of images at fixed temperature to monitor changes of the speckle pattern and this was repeated for different temperatures. No magnetic field was applied during the experiment.

Figure 1(a) shows the magnetic force microscopy (MFM) image of the sample at 300 K. An estimate from the MFM image puts the domain size to be about 120 nm which corresponds to  $\mathbf{q}_{\text{domain}} = 5 \times 10^{-3} \text{ \AA}^{-1}$ . Figure 1(c) shows a line cut of the data obtained after time averaging along the  $\mathbf{q}_x$  direction at  $T=300 \text{ K}$  (in-plane magnetization). Due to intensity limitation the maximum  $\mathbf{q}$  that we could reach is  $3 \times 10^{-4} \text{ \AA}^{-1}$  which means we accessed only some of the Fourier components of the magnetic signal away from  $\mathbf{q}_{\text{domain}}$ . Thus, our signal is dominated by charge roughness scattering with a weak magnetic signal riding on top of it and we are mainly probing  $\mathbf{q} \rightarrow 0$  limit of the in-plane magnetic structure.

A Lorentzian fit to the curve [solid line in Fig. 1(c)] puts the correlation length to be about 1500 nm. We have not seen any significant change in the line shape as the temperature is lowered to 150 K which would be indicative of a change in domain pattern or size. A large variation in domain configuration is seen in systems where SRT is observed as the thickness is changed with the domain size getting smaller as the SRT is approached. On the other hand the Au/Co/Au sample that we use is tailored to exhibit temperature-dependent SRT. The temperature change from 150–300 K, which is about 100 K variation around  $T_{\text{SRT}}$ , is a perturbative change to the overall energy. It is therefore likely that small disordered

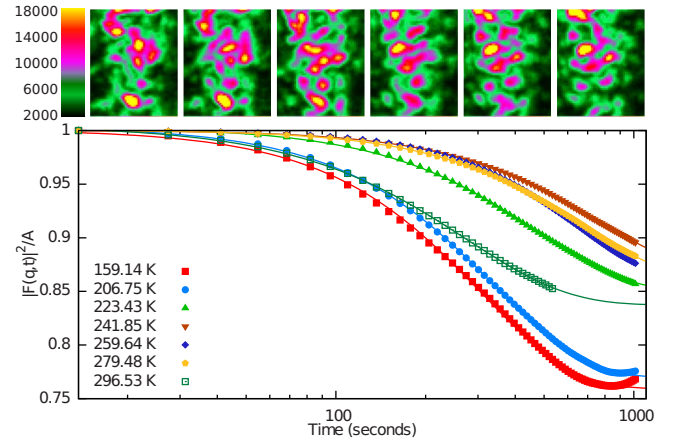


FIG. 2. (Color online) Top Panel: false color plot of the speckle pattern. The images are separated in time by 410.5 s. Plot of the intermediate scattering function  $F(\mathbf{q}, t)$  as a function of temperature for  $\mathbf{q} = 2.58 \times 10^{-4} \text{ \AA}^{-1}$ . The curves are normalized by the speckle contrast  $A$ . The lines are fits to the data. The form of the fit is a stretched exponential and is discussed in the text.

domain structure is maintained through out our measured temperature range.

The speckle patterns are analyzed using the intensity-intensity temporal autocorrelation function  $g_2$  which is defined as

$$g_2(\mathbf{q}, t) = \frac{\langle I(\mathbf{q}, t') I(\mathbf{q}, t' + t) \rangle_{t'}}{\langle I(\mathbf{q}, t) \rangle_{\mathbf{q}, t'}^2} = 1 + A |F(\mathbf{q}, t)|^2, \quad (1)$$

where  $I(\mathbf{q})$  is the intensity at wave vector  $\mathbf{q}$ ,  $t$  is the time delay, and brackets represents averages over the subscripted variables  $\mathbf{q}'$  and  $t'$ .  $F(\mathbf{q}, t)$  is the intermediate scattering function and  $A$  is the speckle contrast that is determined by the beam coherence, among other things.

The top panel of Fig. 2 shows the time evolution of the speckle pattern taken at  $T=279.5 \text{ K}$ . Each image is a 10 s. exposure of the same region and separated in time by 410.5 s. The changes in the speckle pattern with time are indicative of slow fluctuations in the magnetic structure on the order of hundreds of seconds. Figure 2 shows  $|F(\mathbf{q}, t)|^2$  for  $\mathbf{q} = 2.58 \times 10^{-4} \text{ \AA}^{-1}$  as a function of temperature. Repeated attempts to fit the data with a power law or logarithmic time which might suggest glassy dynamics or domain growth were unsuccessful. Rather the data were found to agree best with a stretched exponential of the form

$$|F(\mathbf{q}, t)|^2 \propto \exp[-(t/\tau)^\beta], \quad (2)$$

where  $\tau$  is the characteristic decay constant and  $\beta$  is the stretching exponent. Within our measurement time, we have not seen the autocorrelation curve go to a fully decorrelated state. This is because a significant amount of speckle intensity is due to the frozen-in charge disorder which is always self-correlated. Figure 3 shows the measured decay constants extracted from the fitted  $g_2$  functions for four different  $\mathbf{q}$  values. The time scale of magnetization fluctuations exhibits a dramatic maximum as the temperature transits the SRT. The fitted values of the stretching exponent  $\beta$  (inset of Fig.

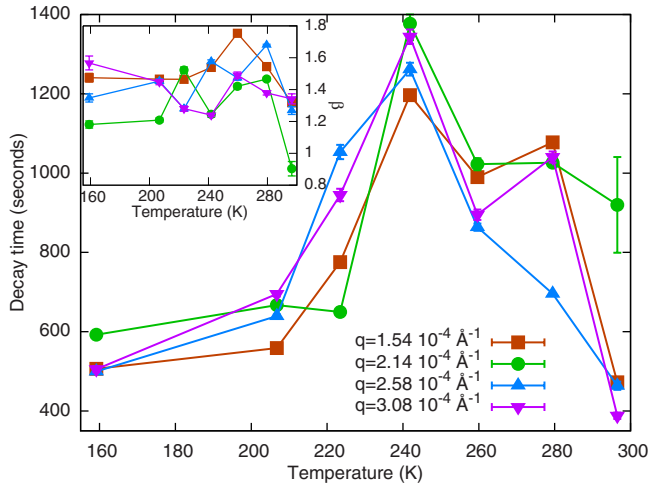


FIG. 3. (Color online) Extracted decay times as a function of temperature. The lines are a guide for the eye. There is an increase in the decay time at the spin-reorientation transition. Inset shows the stretching exponent  $\beta$  as a function of temperature.

3) are typically greater than unity but do not show any systematic variation as a function of temperature.

A value of  $\beta > 1$  has been observed for a myriad of systems both in soft condensed matter as well as magnetic systems and signifies solidlike collective motion.<sup>14,15</sup> With  $\beta > 1$  providing an excellent fit to our results, it is clear that the slow, mesoscale magnetization fluctuations associated with an SRT are characterized by collective dynamics over the entire temperature range measured. Previously, measurements of the driven macroscopic magnetization relaxation in a similar SRT system observed a simple exponential decay.<sup>24</sup> Not surprisingly, the thermally driven mesoscale magnetization fluctuations near an SRT are more complex than might be predicted from measurements of macroscale dissipation. It will be important to connect these two regimes by probing at smaller scattering wave vector in the future.

Figure 4 shows the anisotropy space phase diagram<sup>25</sup> wherein we plot the relationship between the first- and second-order anisotropies. We use  $\tilde{K}_1(T) = K_1(T) - 2\pi M_s(T)^2$  and  $K_2(T)$  as the temperature-dependent anisotropy constants,  $M_s(T)$  is the saturation magnetization, which we approximate as  $M_s(T) = M_0(1 - T/T_C)^\beta$ , with the  $\beta$  value corresponding to a two-dimensional XY model<sup>26</sup> and  $T_C$  as the Curie temperature.  $K_1(T)$  and  $K_2(T)$  are related to magnetization by  $K(T) = K_0[M_s(T)/M_0]^n$ , where  $n=3$  and  $n=10$  for  $K_1(T)$  and  $K_2(T)$ , respectively.<sup>27</sup> Combining these functional dependencies with measured values of  $K_1(300 \text{ K}) = 11.9 \times 10^6 \text{ erg/cm}^3$  (Ref. 7) and  $K_2(300 \text{ K}) = 6.3 \times 10^6 \text{ erg/cm}^3$ ,<sup>28</sup> the temperature-dependent anisotropy curves are determined.  $T_C$  was set to 500 K such that  $\tilde{K}_1(T) = 0$  and the SRT temperature matches what is observed from superconducting quantum interference device (SQUID) measurements in Fig. 1(d). The anisotropy space traversed by our Au/Co/Au sample when the temperature is varied is shown by the dotted line curve in Fig. 4 with arrows to show the temperatures between which the canted phase is expected. We note that because we are using a published value of  $K_2(T)$  the actual value for this system may be slightly

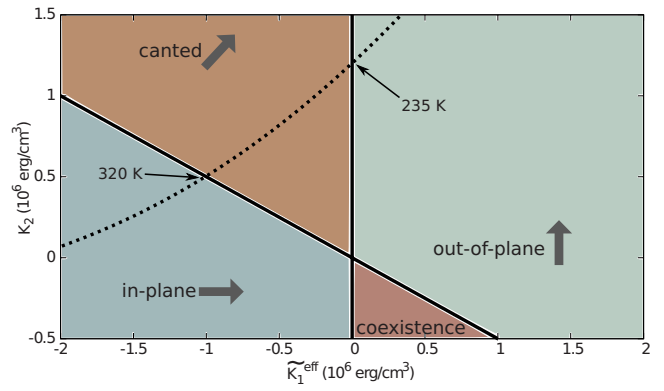


FIG. 4. (Color online) Plot of  $\tilde{K}_1(T)$  vs  $K_2(T)$ . The dotted line indicates the path traversed in the anisotropy space by the Au/Co/Au system when the temperature is changed. The arrows indicate the temperature where the magnetization is fully in-plane or out-of-plane state.

different but it is well known that  $K_2(T) > 0$  for Co (Ref. 29) and conclusion that this system goes through a continuous transition still holds. Changing the value of  $K_2(T)$  shifts the dotted curve vertically in Fig. 4 without changing the nature of transition.

The simple model provides a decent, though not perfect, description of the SRT phase diagram. The first important feature of this model is that  $K_2(T) > 0$  through the entire SRT, in which case the Landau theory predicts a continuous phase transition in which the magnetization angle  $\theta$  cants continuously between  $\theta=0$  at  $T_1$  defined by  $\tilde{K}_1(T)=0$  and  $\theta=90^\circ$  at  $T_2$  defined by  $K_2(T) = -K_1(T)/2$  (the solid line with negative slope in Fig. 4). Our phase diagram therefore indicates that for the Au/Co/Au system, the phase transition occurs through a cone state and does not occur through a coexisting in-plane or out-of-plane domain state. Near the transition the energy minimum is relatively flat. The number of thermally accessible states increases dramatically in this regime<sup>30</sup> and this causes thermal fluctuations to be long lived. This language is reminiscent of the critical slowing observed for systems exhibiting second-order phase transitions but the analogy should not be taken too far. We wish to note here that together with  $\tilde{K}_1(T)=0$  and the fact that the stretched exponential is greater than unity in Fig. 2, suggest that the phases near the SRT exhibit complex short-range order spatiotemporal correlations.

The conclusion that the SRT proceeds through a canted phase relies on the reported positive value of  $K_2(T)$  at 300 K. If  $K_2(T) < 0$ , a transition through a mixed phase comprised of domains of in-plane and out-of-plane magnetization would be predicted, and this structure might well lead to complex fluctuations brought upon by the broadening in-plane (out-of-plane) domain that annihilate the out-of-plane (in-plane) domains.<sup>31</sup> The simplest Landau theory does not include the possibility of domains in the canted phase. However, given the very low in-plane anisotropy of hexagonal cobalt, it is certainly plausible that exotic, fluctuating domains exist in the canted phase with average in-plane magnetization vanishing at zero applied field.<sup>12,13</sup> Finally, the increasing so-

phistication of magnetic film growth offers the tantalizing possibility of tuning the  $K_1(T) - K_2(T)$  curve in Fig. 4 so that it passes through the origin where both  $\widetilde{K}_1(T)$  and  $K_2(T)$  vanish. Further interesting phase behaviors might then be observed.

The authors acknowledge J. D. Thompson of the Los Alamos National Laboratory for helping in the magnetometry measurements. This work at ALS/LBNL was supported by

the Director, Office of Science, Office of Basic Energy Sciences, of the U.S. Department of Energy under Contract No. DE-AC02-05CH11231. Work in the group of SDK at U. Oregon was supported by NSF under Grant No. DMR-0506241. Work in the group of CMF at U. Arizona was supported by DOE under Grant No. DE-FG02-93ER45488. S.P. acknowledges support from KOSEF under Grants No. R01-2008-000-21092-0 and No. 2009-0083140.

---

\*Author to whom correspondence should be addressed; SRoy@lbl.gov

- <sup>1</sup>R. Allenspach and A. Bischof, *Phys. Rev. Lett.* **69**, 3385 (1992).
- <sup>2</sup>R. Sellmann, H. Fritzsche, H. Maletta, V. Leiner, and R. Siebrecht, *Phys. Rev. B* **64**, 054418 (2001).
- <sup>3</sup>B. N. Engel, C. D. England, R. A. Van Leeuwen, M. H. Wiedmann, and C. M. Falco, *Phys. Rev. Lett.* **67**, 1910 (1991).
- <sup>4</sup>H. L. Meyerheim, D. Sander, R. Popescu, J. Kirschner, O. Robach, and S. Ferrer, *Phys. Rev. Lett.* **93**, 156105 (2004).
- <sup>5</sup>R. Vollmer, Th. Gutjahr-Loser, J. Kirschner, S. van Dijken, and B. Poelsema, *Phys. Rev. B* **60**, 6277 (1999).
- <sup>6</sup>Y.-P. Zhao, G. Palasantzas, G.-C. Wang, and J. Th. M. De Hosson, *Phys. Rev. B* **60**, 1216 (1999).
- <sup>7</sup>S. Park, X. Zhang, A. Misra, J. D. Thompson, M. R. Fitzsimmons, S. Lee, and C. M. Falco, *Appl. Phys. Lett.* **86**, 042504 (2005).
- <sup>8</sup>C. A. F. Vaz, J. A. C. Bland, and G. Lauhoff, *Rep. Prog. Phys.* **71**, 056501 (2008).
- <sup>9</sup>A. Kashuba and V. L. Pokrovsky, *Phys. Rev. Lett.* **70**, 3155 (1993).
- <sup>10</sup>J. Choi, J. Wu, C. Won, Y. Z. Wu, A. Scholl, A. Doran, T. Owens, and Z. Q. Qiu, *Phys. Rev. Lett.* **98**, 207205 (2007).
- <sup>11</sup>M. Speckmann, H. P. Oepen, and H. Ibach, *Phys. Rev. Lett.* **75**, 2035 (1995).
- <sup>12</sup>L. Louail, K. Ounadjela, and R. L. Stamps, *J. Magn. Magn. Mater.* **167**, L189 (1997).
- <sup>13</sup>R. Frömter, H. Stillrich, C. Menk, and H. P. Oepen, *Phys. Rev. Lett.* **100**, 207202 (2008).
- <sup>14</sup>P. Falus, M. A. Borthwick, S. Narayanan, A. R. Sandy, and S. G. J. Mochrie, *Phys. Rev. Lett.* **97**, 066102 (2006).
- <sup>15</sup>O. G. Shpyrko *et al.*, *Nature (London)* **447**, 68 (2007).
- <sup>16</sup>M. S. Pierce and C. R. Buechler *et al.*, *Phys. Rev. Lett.* **94**, 017202 (2005).
- <sup>17</sup>S. Eisebitt and J. Lüning *et al.*, *Nature (London)* **432**, 885 (2004).
- <sup>18</sup>J. J. Turner and K. J. Thomas *et al.*, *New J. Phys.* **10**, 053023 (2008).
- <sup>19</sup>K. Chesnel, M. Belakhovsky, F. Livet, S. P. Collins, G. van der Laan, S. S. Dhesi, J. P. Attane, and A. Marty, *Phys. Rev. B* **66**, 172404 (2002).
- <sup>20</sup>G. van der Laan, *Physica B* **345**, 137 (2004).
- <sup>21</sup>G. Grübel and F. Zontone, *J. Alloys Compd.* **362**, 3 (2004).
- <sup>22</sup>K. Chesnel, J. J. Turner, M. Pfeifer, and S. D. Kevan, *Appl. Phys. A: Mater. Sci. Process.* **92**, 431 (2008).
- <sup>23</sup>J. B. Kortright and S.-K. Kim, *Phys. Rev. B* **62**, 12216 (2000).
- <sup>24</sup>A. Berger and H. Hopster, *Phys. Rev. Lett.* **76**, 519 (1996).
- <sup>25</sup>H. P. Oepen, M. Speckmann, Y. Millev, and J. Kirschner, *Phys. Rev. B* **55**, 2752 (1997).
- <sup>26</sup>J. S. Tsay, H. Y. Nieh, Y. D. Yao, Y. T. Chen, and W. C. Cheng, *Surf. Sci.* **566-568**, 226 (2004).
- <sup>27</sup>W. J. Carr Jr., *Phys. Rev.* **109**, 1971 (1958).
- <sup>28</sup>A. Murayama, K. Hyomi, J. Eickmann, and C. M. Falco, *Phys. Rev. B* **58**, 8596 (1998).
- <sup>29</sup>C. Chappert, K. L. Dang, P. Beauvillain, H. Hurdequint, and D. Renard, *Phys. Rev. B* **34**, 3192 (1986).
- <sup>30</sup>K. P. Belov, A. K. Zvezdin, A. M. Kadomtseva, and R. Z. Levitin, *Sov. Phys. Usp.* **19**, 574 (1976).
- <sup>31</sup>E. Bauer, T. Duden, and R. Zdyb, *J. Phys. D* **35**, 2327 (2002).